FUNDAMENTALS & APPLICATIONS

CHEMELECTROCHEM

ANALYSIS & CATALYSIS, BIO & NANO, ENERGY & MORE

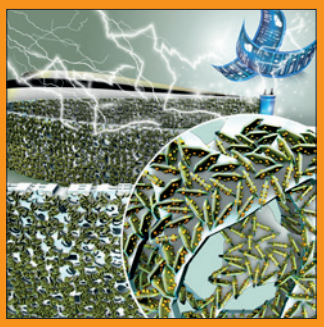
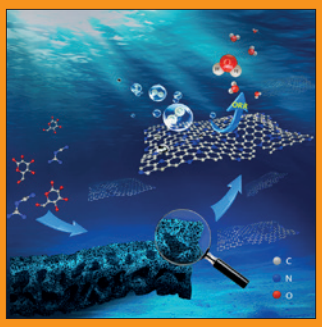
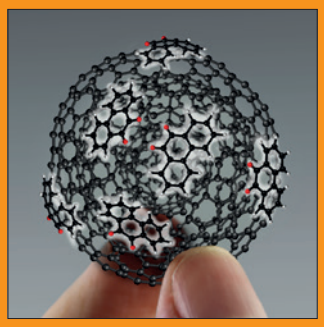
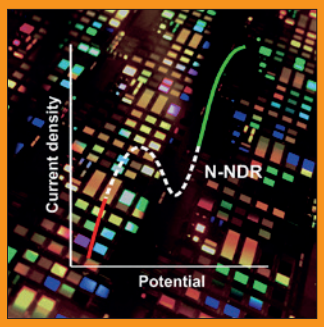

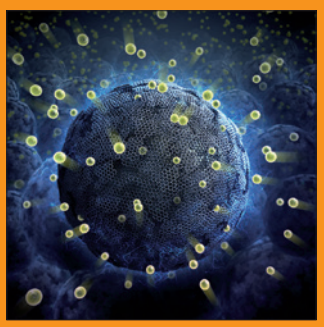



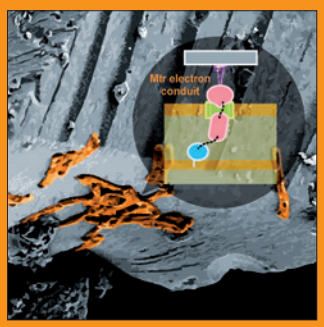

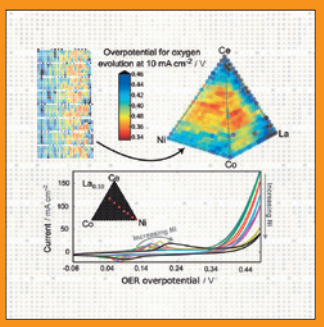

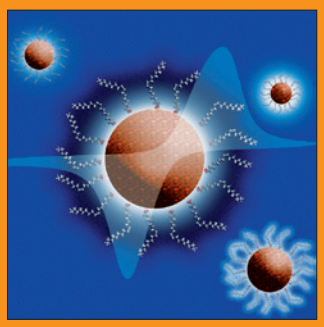
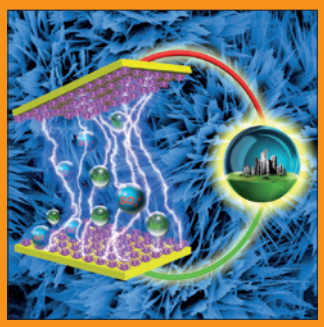
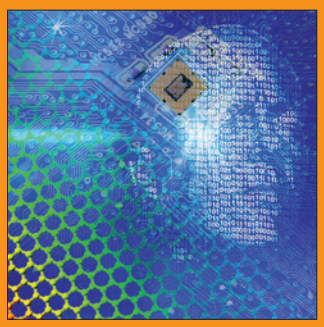

Reprint

A Journal of

WILEY-VCH

www.chemelectrochem.org

ChemPubSoc Europe

ChemPubSoc Europe

DOI: 10.1002/celc.201900482

CHEMELECTROCHEM Articles

Heterostructured Bismuth Vanadate/Cobalt Phosphate Photoelectrodes Promote TEMPO-Mediated Oxidation of 5-Hydroxymethylfurfural

David J. Chadderdon,[a] Li-Pin Wu,[a] Zachary A. McGraw,[a] Matthew Panthani,*[a] and Wenzhen Li*[a, b]

Motivated by replacing the kinetically unfavorable oxygen evolution reaction (OER) and producing value-added products in photoelectrochemical cells (PECs), we report that bismuth vanadate ($BiVO_4$) photoelectrodes modified with a cobalt phosphate (CoPi) overlayer facilitate 2,2,6,6-tetramethylpiperidine-1-oxyl (TEMPO)-mediated selective oxidation of 5-hydroxymethylfurfural (HMF). CoPi layers with sufficient thickness were found to reduce the potential required for TEMPO oxidation by 0.5 V, as well as increase charge injection efficiency sevenfold compared to $BiVO_4$ without CoPi. Furthermore, the undesired OER was completely suppressed when using the heterostructured photoanodes. Transient photocurrent measurements suggested that CoPi alleviates recombination losses resulting from the back reduction of oxidized TEMPO. The PECs with $BiVO_4$/CoPi bilayer achieved 88% yield to 2,5-furandicarboxylic acid (FDCA) from HMF oxidation under mild conditions, whereas <1% FDCA was generated with $BiVO_4$. These findings suggest that suppression of the back reduction process substantially improves the efficiency of the oxidation, giving a potential route to more efficient solar fuel/chemical production.

1. Introduction

Photoelectrochemistry has a key role in moving our society toward a sustainable energy future. PECs use light-absorbing semiconductor photoelectrodes to drive reactions with solar energy, often aided by external electricity input which can be supplied from renewable sources. In typical PECs, low-value molecules such as H_2O or CO_2 are reduced at metal/semiconductor cathodes to generate hydrogen gas (i.e., the hydrogen evolution reaction, HER) or carbon-based fuels and chemicals.[1] However, such PECs commonly suffer from poor energy conversion efficiency. This can largely be attributed to the slow kinetics and large overpotentials associated with the OER that occurs at the anode. Platinum-group metal catalysts are generally used to overcome the kinetic limitations; however, the high cost and low abundance of these materials limit their large-scale application.[2] Furthermore, the oxygen produced at the anode is not valuable. Therefore, it is desirable to find a more favorable anode reaction that utilizes low-cost and Earth-abundant electrode materials, and that generates value-added products.

A promising approach to improve the feasibility of PECs and related electrochemical cells is to pair HER at the cathode with anodic oxidation of biomass-derived chemicals (e.g., alcohols and aldehydes).[3] Alcohol oxidation is thermodynamically favorable compared to OER,[4] therefore having the potential to reduce operating cell voltages and improve energy efficiency. Moreover, electrochemical alcohol oxidation can be tuned to selectively target desired chemicals,[5] enabling the generation of high-purity valuable products from renewable carbon sources. For example, 5-hydroxymethylfurfural (HMF), a platform molecule derived from C6 carbohydrates,[6] can be selectively oxidized to 2,5-furandicarboxylic acid (FDCA), a valuable precursor for biobased polymers.[7] In a breakthrough study, Cha et al. demonstrated the photoelectrochemical conversion of HMF to FDCA using a bismuth vanadate ($BiVO_4$) photoanode and a homogeneous redox mediator, TEMPO (2,2,6,6-tetramethylpiperidine-1-oxyl).[3a] This work achieved remarkable selectivity and faradaic efficiency; however, a considerable external bias was required to support separation of photogenerated charge carriers and achieve high photocurrent densities. Although $BiVO_4$ has emerged as one of the most promising metal oxide-based photoanodes for OER,[8] it has been established that surface modifications, for example with catalysts such as cobalt phosphate (CoPi),[9] Co_3O_4,[10] or transition metal oxyhydroxides,[11] are required to mitigate charge recombination losses. However, such modifications have not been applied to $BiVO_4$ photoanodes for enhancing redox-mediated alcohol oxidations because it was presumed that they would promote OER in favor over mediator oxidation.[3a,12]

In this study, we challenge these previous presumptions by showing that $BiVO_4$ photoanodes modified with CoPi, a well-known OER electrocatalyst, can be tailored to enhance TEMPO-mediated alcohol oxidation over OER (water oxidation). We

[a] D. J. Chadderdon, L.-P. Wu, Z. A. McGraw, Prof. Dr. M. Panthani, Prof. Dr. W. Li
Department of Chemical & Biological Engineering
Iowa State University
Ames, IA 50011 (USA)
E-mail: wzli@iastate.edu
panthani@iastate.edu
[b] Prof. Dr. W. Li
US Department of Energy Ames Laboratory
Ames, IA 50011 (USA)

Supporting information for this article is available on the WWW under https://doi.org/10.1002/celc.201900482

demonstrate for heterostructured $BiVO_4$/CoPi photoanodes that OER activity is sensitive to CoPi electrodeposition time: short times (e.g. 1 min) reduce the onset potential and increase photocurrent for OER, whereas longer depositions severely suppress OER activity. We exploit the latter phenomenon to oxidize TEMPO without any faradaic efficiency loss to OER. Furthermore, TEMPO oxidation is enhanced for $BiVO_4$/CoPi photoanodes in terms of reduced onset potential and increased photocurrent compared to $BiVO_4$. Transient photocurrent measurements provide insight into interfacial charge transfer and recombination processes, elucidating the likely role of CoPi. Finally, we use $BiVO_4$/CoPi photoanodes to drive TEMPO-mediated oxidation of HMF to FDCA and demonstrate the viability of using heterostructured photoanodes for efficient biomass upgrading in PECs.

2. Results and Discussion

2.1. Physical Characterization of $BiVO_4$ Films

$BiVO_4$ films were synthesized on fluorine-doped tin oxide (FTO) glass substrates by electrodeposition and thermal processing using a previously reported method.[11c] Scanning electron microscopy (SEM) revealed the $BiVO_4$ films were nanoporous and about 2 μm thick (Figure 1). Energy-dispersive spectroscopy

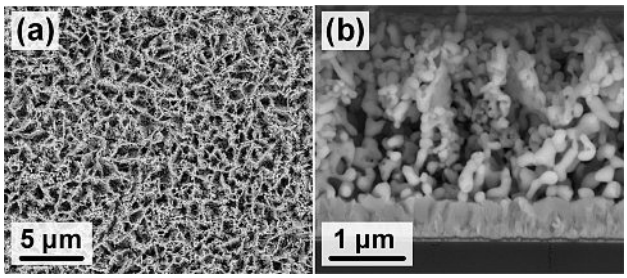

Figure 1. SEM images of $BiVO_4$ films on FTO glass including a) top and b) cross-sectional views.

(EDS) confirmed the composition of the films and indicated a Bi/V ratio of approximately 1:1 (Table S1). X-ray diffraction (XRD) patterns were consistent with a monoclinic $BiVO_4$ crystal structure (Figure S1). UV-vis diffuse absorbance spectra and corresponding Tauc analysis (Figure S2) confirmed a bandgap of about 2.47 eV, which matches those reported in literature.[13]

2.2. Photoelectrochemical Measurements

Photoelectrochemical measurements were performed in sodium borate electrolytes (pH 9.2) under simulated solar illumination (AM1.5, 100 mW cm^{-2}). Figure 2 shows the linear sweep voltammogram (LSV) for $BiVO_4$ in electrolyte containing sodium sulfite, which is known to be a good hole scavenger,[14] and is expected to extract nearly all photogenerated holes that reach

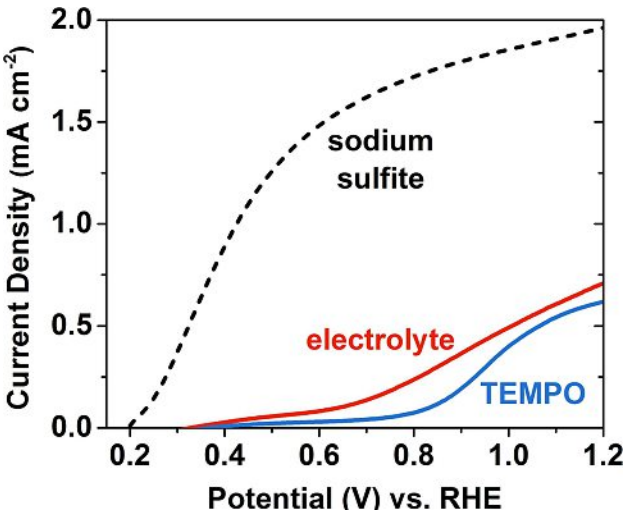

Figure 2. LSV with AM1.5 illumination for $BiVO_4$ photoanodes in electrolytes with or without 5.0 mM TEMPO or 0.2 M sodium sulfite

the semiconductor/electrolyte interface. Thus, the sulfite oxidation photocurrent density ($j_{sulfite}$) provides an estimate for the total rate of holes reaching the interface. For TEMPO-mediated oxidations, it is desirable that a photoanode facilitates TEMPO oxidation at low potentials but has poor activity for OER, the main competing oxidation reaction in aqueous electrolytes.[15] Figure 2 shows the LSV collected in electrolyte without sulfite, in which case the majority of the photocurrent is from OER. The onset potential for OER was increased by about 150 mV compared to that for sulfite oxidation, and the photocurrent density (j_{OER}) was remarkably lower than $j_{sulfite}$. The net charge injection efficiency (the fraction of surface-reaching holes that are utilized for oxidation of species in the electrolyte) was estimated by the ratio $j_{OER}/j_{sulfite}$ to be 6.3% at 0.64 V. This suggests that the vast majority of the surface-reaching holes were lost to recombination processes. The photocurrent was even lower with TEMPO present in the electrolyte; most notably in the low potential region (i.e. $<$ 1.0 V).

2.3. Physical Characterization and Photoelectrochemical Performance of $BiVO_4$/CoPi

CoPi was deposited onto $BiVO_4$ electrodes using the electrodeposition method described by Kanan and Nocera.[16] Briefly, CoPi was electrodeposited from a solution of cobalt(II) nitrate (0.5 mM) and potassium phosphate (0.1 M, pH 7.0) at 1.1 V versus a Ag/AgCl reference electrode. Deposition time was varied between 1 and 30 min to obtain a range of CoPi loadings. A typical current density versus time plot for CoPi deposition is shown in Figure S3. XRD patterns of $BiVO_4$/CoPi did not change as compared with $BiVO_4$ as shown in Figure S1, while SEM analysis revealed that CoPi deposition had no effect on film morphology (Figure S4), suggesting that the deposition was uniform over the electrode. The Co/P atomic ratio estimated by EDS was approximately 1.9:1.0, which is consis-

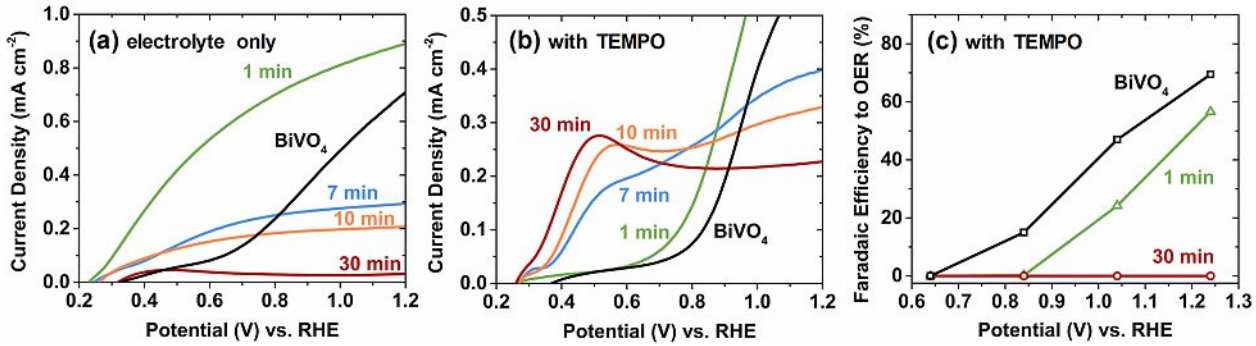

Figure 3. LSVs with AM1.5 illumination for $BiVO_4$ and $BiVO_4$/CoPi photoanodes with varying CoPi deposition times (denoted within figures) in electrolyte a) without TEMPO and b) with 5.0 mM TEMPO. c) Calculated faradaic efficiency to OER in electrolyte with 5.0 mM TEMPO.

tent with previous reports.[16] There was no appreciable change in the UV-vis-NIR absorption spectrum, indicating that inclusion of CoPi did not affect light absorption properties of the photoanode.

Modifying $BiVO_4$ with a relatively thin CoPi overlayer (i.e. 1 deposition time) reduced the onset potential and increased photocurrent by about 4.8-fold at 0.64 V for OER compared to $BiVO_4$ (Figure 3a). However, longer depositions suppressed OER; photocurrent for $BiVO_4$/CoPi-30 (i.e. $BiVO_4$ with 30 min CoPi deposition) was reduced by 95% compared to $BiVO_4$ at 1.04 V. The suppression of OER when using thicker CoPi overlayers is consistent with previous reports, which suggested that thicker CoPi overlayers on photoanodes could result in low OER performance due to increased interfacial recombination of conduction band electrons with accumulated CoPi holes,[17] or recombination via direct shunting of CoPi to the conductive back contact (i.e. FTO).[18]

Even though OER was suppressed by thicker CoPi overlayers, we found that photocurrent for TEMPO oxidation was substantially enhanced with increased CoPi deposition times (Figure 3b). This suggests that TEMPO oxidation was able to compete with CoPi-induced charge recombination pathways. For $BiVO_4$/CoPi-30, the potential required for TEMPO oxidation was reduced by nearly 0.5 V (e.g. reduced 475 mV at 0.1 mA cm^{-2}) relative to unmodified $BiVO_4$. Increasing CoPi deposition time beyond 30 min did not lead to further enhancement.

The faradaic efficiency for OER was determined by quantifying evolved O_2 under steady-state conditions (Figure 3c). As a control experiment, the measured and theoretical amounts of O_2 produced were shown to be in good agreement when TEMPO was not present in the electrolyte (Figure S5). Figure 3c shown that OER did not contribute to the photocurrents at 0.64 V; therefore the major contribution to current at this potential can reasonably be assigned to TEMPO oxidation (j_{TEMPO}). The net charge injection efficiency for TEMPO oxidation ($j_{TEMPO}/j_{sulfite}$) at 0.64 V was 15.4% for $BiVO_4$/CoPi-30, a seven-fold increase compared to $BiVO_4$ (2.1%). OER was favorable at higher potentials for unmodified $BiVO_4$ and $BiVO_4$/CoPi prepared with short CoPi deposition times; the faradaic efficiencies to OER at 1.24 V were 70% for $BiVO_4$ and 57% for $BiVO_4$/CoPi with 1 min deposition. This was likely due to mass transport limitations for TEMPO oxidation at higher potentials. Remarkably, O_2 was not detected for $BiVO_4$/CoPi-30 in electrolytes containing TEMPO at any potential tested. These findings show that the $BiVO_4$/CoPi-30 photoanode has greater selectivity towards TEMPO oxidation compared to $BiVO_4$, thus completely suppressing undesired OER (below detection limit).

The negligible OER faradaic efficiencies observed at lower potentials in electrolytes with TEMPO (e.g. ~0% at 0.64 V) indicate that TEMPO oxidation was kinetically favored over OER. However, the photocurrent for $BiVO_4$ in electrolytes with TEMPO was actually lower than in electrolytes without TEMPO (e.g. ~67% lower at 0.64 V). These seemingly inconsistent observations gave rise to a hypothesis that photocurrents were not limited by slow TEMPO oxidation kinetics, but by other factors. By extension, it is very unlikely that the higher TEMPO oxidation photocurrents observed for $BiVO_4$/CoPi-30 resulted from enhanced charge transfer kinetics (i.e. electrocatalysis).

Photocurrents for $BiVO_4$ may have been limited by solution-mediated charge recombination via the back reduction of oxidized TEMPO ($TEMPO^+$), as depicted in Figure 4a. In principle, back reduction can occur by transfer of electrons from the conduction band or surface states of the semiconductor, or from the conductive substrate (e.g. FTO).[19] Cyclic voltammo-

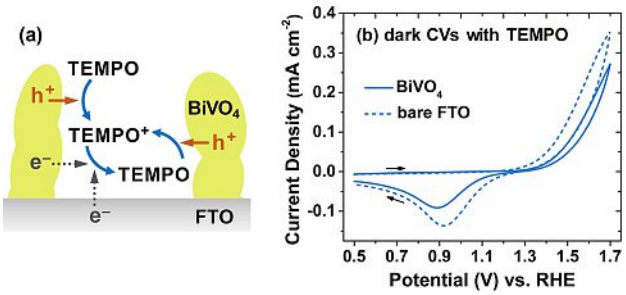

Figure 4. a) Depiction of possible solution-mediated charge recombination pathways. Photogenerated holes oxidize TEMPO to $TEMPO^+$, which may be reduced back to TEMPO via electron transfer from the $BiVO_4$ conduction band or surface states, or from the exposed FTO substrate. b) Dark cyclic voltammograms (CVs) for $BiVO_4$ or bare FTO electrodes in electrolyte with 5.0 mM TEMPO.

grams measured in the dark revealed that TEMPO exhibits quasi-reversible electrochemical oxidation/reduction on unmodified $BiVO_4$ and bare FTO electrodes (Figure 4b). The midpoint potential was around 1.28 V, indicating that $TEMPO^+$ is susceptible to electrochemical reduction over most of the potential range of interest for photoelectrochemical TEMPO oxidation. In the dark, the low concentration of holes in n-type semiconductors (such as $BiVO_4$) prevents them from facilitating oxidations.[20] Accordingly, the dark oxidation current observed for $BiVO_4$ electrodes can be attributed mainly to the underlying FTO substrate.[21] The dark oxidation currents for $BiVO_4$ and bare FTO were of similar magnitudes, suggesting that a substantial fraction of the underlying FTO was accessible to the electrolyte through the nanoporous $BiVO_4$ films. Therefore, the exposed FTO could potentially facilitate electrochemical back reduction of $TEMPO^+$ at potentials more negative than 1.28 V.

2.4. Transient Photocurrent Measurements

We used transient photocurrent measurements to test our hypothesis and gain more insight about charge transfer and recombination dynamics. Figure 5a shows LSVs for $BiVO_4$ under chopped AM1.5 illumination. In pure electrolyte (i.e. without TEMPO), transient current spikes were observed upon light "on" and "off", which are generally assigned to the back recombination of electrons with accumulated holes.[22] The spikes were most prominent at low potentials and diminished at increasingly anodic potentials. Negative transient current was negligible at potentials greater than ~0.8 V. This behavior has been attributed to enhanced band bending and charge separation at strongly anodic potentials.[23] The positive and negative current spikes were more pronounced in electrolyte containing TEMPO. Notably, we observed large negative current spikes (not observed in pure electrolyte) that initiated around 0.6 V and persisted up to about 1.2 V. Within that same potential range, the anodic photocurrents decayed to values lower than in pure electrolyte. We attribute this transient behavior to the electrochemical back reduction of $TEMPO^+$, which is operable over this potential range (cf. Figure 4b).

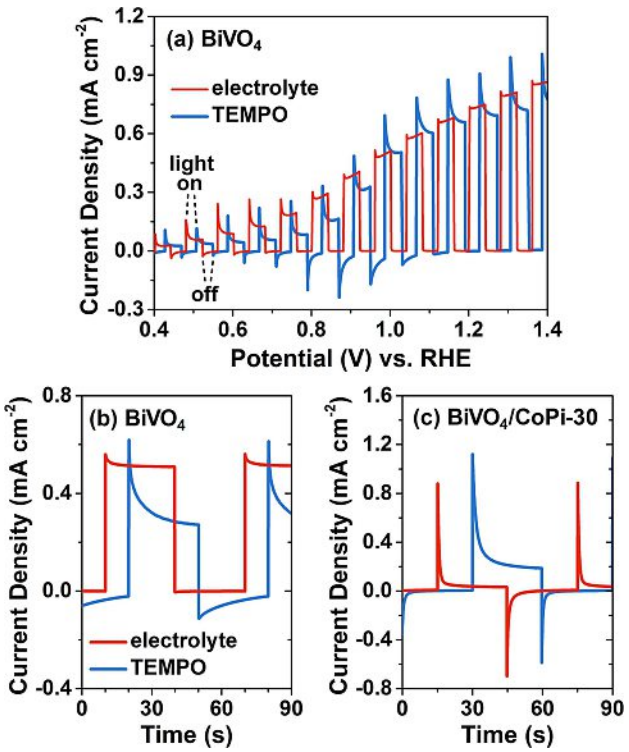

Figure 5. Transient photocurrent measurements with chopped AM1.5 illumination. a) LSVs for $BiVO_4$ in pure electrolyte and electrolyte with 5.0 mM TEMPO. b, c) Transient photocurrents at 1.04 V vs. RHE for $BiVO_4$ and $BiVO_4$/CoPi-30, respectively. For clarity, the traces in (b) and (c) are offset with respect to time.

Figure 5b and 5c show transient photocurrent measurements for $BiVO_4$ and $BiVO_4$/CoPi-30 at a fixed potential of 1.04 V. $BiVO_4$ displayed behavior consistent with the LSVs under chopped illumination; quasi-steady-state photocurrents were smaller and negative transient currents were much larger for electrolytes with TEMPO compared to pure electrolytes. The negative current decayed very slowly ($t_{1/2} \approx 13$ s) and did not reach steady state during the dark periods. As previously mentioned, we assign the negative current mainly to the back reduction of $TEMPO^+$ that accumulates in solution during illuminated periods. In pure electrolyte, $BiVO_4$/CoPi-30 exhibited high anodic current initially after illumination; however, the photocurrent rapidly decayed to nearly zero. We also observed sharp negative transients, upon turning off illumination. This behavior has been attributed to CoPi oxidation by photogenerated holes and subsequent back recombination of electrons with accumulated oxidized CoPi species.[24] In electrolytes with TEMPO, quasi-steady-state anodic current was greatly increased (i.e. ~six-fold) and the negative transient current was diminished compared to pure electrolytes. Most notably, the slowly-decaying negative current assigned to $TEMPO^+$ back reduction was not observed for $BiVO_4$/CoPi-30. Based on this information, the enhanced TEMPO oxidation photocurrents for CoPi-modified $BiVO_4$ photoanodes most likely arises from the CoPi layer inhibiting solution-mediated charge recombination.

2.5. TEMPO-Mediated Oxidation of Biorenewable HMF

Finally, we used the $BiVO_4$/CoPi photoelectrodes for TEMPO-mediated oxidation of biomass-derived HMF. Due to its high value for biomass conversion, we targeted HMF as an exemplary multifunctional substrate containing both alcohol and aldehyde functionalities (Figure 6a). LSVs for $BiVO_4$/CoPi-30 show that photocurrent increased after adding HMF to a TEMPO-containing electrolyte (Figure 6b), resulting from the regeneration of TEMPO following the reaction between the oxoammonium cation (i.e. $TEMPO^+$) and HMF. No increase was observed in the absence of TEMPO, indicating that the non-mediated HMF oxidation was negligible under these conditions.

TEMPO-mediated photoelectrolysis of HMF was performed at 0.64 V for 2.7 hours. Relatively low HMF conversion (15.2%) and yield to FDCA (~0.1%) were obtained using a $BiVO_4$ photoanode at such a mild potential (Table S3). In sharp

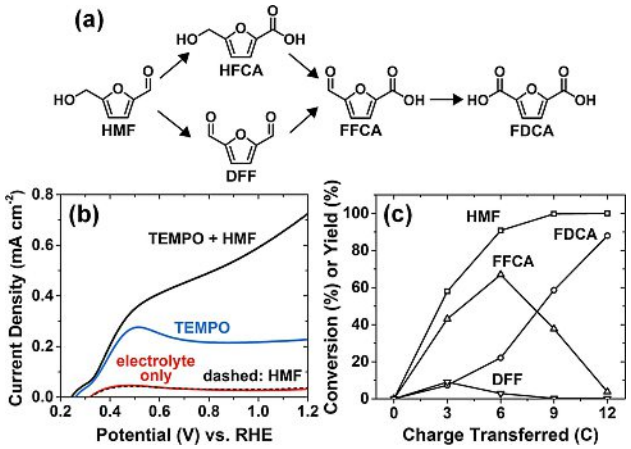

Figure 6. a) Reaction pathways for HMF oxidation to FDCA. b) LSVs under AM1.5 illumination for $BiVO_4$/CoPi-30 in electrolyte only, electrolyte with 5.0 mM TEMPO, electrolyte with 5.0 mM TEMPO and 5.0 mM HMF, and electrolyte with 5.0 mM HMF without TEMPO. c) HMF conversion and product yields for photoelectrolysis at 0.64 V vs. RHE for $BiVO_4$/CoPi-30.

contrast, $BiVO_4$/CoPi-30 achieved 88% yield to FDCA (Figure 6c), which we attribute to its greatly enhanced TEMPO oxidation performance. We highlight that the role of the photoanode in this system is to oxidize TEMPO to $TEMPO^+$, which then oxidizes the substrate (i.e. HMF) homogeneously in the electrolyte. It has been demonstrated that TEMPO-catalyzed oxidation has broad applicability to different alcohol-containing substrates.[25] Therefore, this approach is not uniquely suited for HMF conversion, but rather we expect it to be readily applicable for the TEMPO-mediated oxidation of a wide range of biologically-derived substrates.

3. Conclusions

In summary, we developed heterostructured photoelectrodes composed of nanoporous $BiVO_4$ films modified with CoPi for TEMPO-mediated alcohol oxidation. CoPi electrodeposition time was a critical parameter for selectively promoting TEMPO oxidation in favor over OER. $BiVO_4$/CoPi prepared by a 30 min CoPi deposition reduced the potential required for TEMPO oxidation by about 0.5 V and greatly enhanced the photocurrents for TEMPO oxidation compared to $BiVO_4$. In situ O_2 measurements confirmed that TEMPO oxidation with $BiVO_4$/CoPi-30 proceeded without any faradaic efficiency loss to OER. Transient photocurrent measurements suggested that CoPi alleviates solution-mediated recombination losses resulting from the back reduction of oxidized TEMPO, which we identified as a major limiting factor for $BiVO_4$ photoanode performance. $BiVO_4$/CoPi-30 facilitated TEMPO-mediated oxidation of HMF, an exemplary biomass-derived alcohol, to FDCA with high yield at mild conditions. This work will promote the development of rationally-designed heterostructured photoanodes and the exploration of new routes to more fully utilize renewable electricity, renewable solar energy, and renewable feedstocks.

Acknowledgements

W.L. and D.C. acknowledge support from the Bailey Research Career Development Award. M.G.P. acknowledges support from the Herbert L. Stiles Faculty Fellowship. The authors thank Warren Straszheim and Scott Schlorholtz of Iowa State University for assistance with SEM and XRD. This work was supported in part by the U.S. Department of Energy, Office of Science, and Office of Workforce Development for Teachers and Scientists (WDTS) under the Science Undergraduate Laboratory Internship (SULI) program. W.L. thanks for his Richard Seagrave Professorship and NSF CBET 1512126, and L.W. is grateful to the DOE for the assistantship and opportunity to participate in the SULI program.

Conflict of Interest

The authors declare no conflict of interest.

Keywords: alcohol oxidation · TEMPO · photoelectrocatalysis · bismuth vanadate · biomass

[1] a) G. Centi, S. Perathoner, *ChemSusChem* **2010**, *3*, 195–208; b) M. G. Walter, E. L. Warren, J. R. McKone, S. W. Boettcher, Q. Mi, E. A. Santori, N. S. Lewis, *Chem. Rev.* **2010**, *110*, 6446–6473; c) D. Kim, K. K. Sakimoto, D. Hong, P. Yang, *Angew. Chem. Int. Ed.* **2015**, *54*, 3259–3266; *Angew. Chem.* **2015**, *127*, 3309–3316.

[2] Y. Jiao, Y. Zheng, M. Jaroniec, S. Z. Qiao, *Chem. Soc. Rev.* **2015**, *44*, 2060–2086.

[3] a) H. G. Cha, K.-S. Choi, *Nat. Chem.* **2015**, *7*, 328–333; b) B. You, X. Liu, X. Liu, Y. Sun, *ACS Catal.* **2017**, 4564–4570; c) B. You, N. Jiang, X. Liu, Y. Sun, *Angew. Chem. Int. Ed.* **2016**, *55*, 9913–9917; *Angew. Chem.* **2016**, *128*, 10067–10071.

[4] a) Y. X. Chen, A. Lavacchi, H. A. Miller, M. Bevilacqua, J. Filippi, M. Innocenti, A. Marchionni, W. Oberhauser, L. Wang, F. Vizza, *Nat. Commun.* **2014**, *5*, 4036; b) J. González-Cobos, S. Baranton, C. Coutanceau, *ChemElectroChem* **2016**, *3*, 1694–1704.

[5] a) A. Zalineeva, A. Serov, M. Padilla, U. Martinez, K. Artyushkova, S. Baranton, C. Coutanceau, P. B. Atanassov, *J. Am. Chem. Soc.* **2014**, *136*, 3937–3945; b) D. J. Chadderdon, L. Xin, J. Qi, B. Brady, J. A. Miller, K. Sun, M. J. Janik, W. Li, *ACS Catal.* **2015**, *5*, 6926–6936.

[6] T. Wang, M. W. Nolte, B. H. Shanks, *Green Chem.* **2014**, *16*, 548–572.

[7] a) J. B. Binder, R. T. Raines, *J. Am. Chem. Soc.* **2009**, *131*, 1979–1985; b) W. P. Dijkman, D. E. Groothuis, M. W. Fraaije, *Angew. Chem. Int. Ed.* **2014**, *53*, 6515–6518; *Angew. Chem.* **2014**, *126*, 6633–6636.

[8] Y. Park, K. J. McDonald, K. S. Choi, *Chem. Soc. Rev.* **2013**, *42*, 2321–2337.

[9] a) D. K. Zhong, S. Choi, D. R. Gamelin, *J. Am. Chem. Soc.* **2011**, *133*, 18370–18377; b) S. K. Pilli, T. E. Furtak, L. D. Brown, T. G. Deutsch, J. A. Turner, A. M. Herring, *Energy Environ. Sci.* **2011**, *4*, 5028–5034; c) F. F. Abdi, N. Firet, R. van de Krol, *ChemCatChem* **2013**, *5*, 490–496; d) C. Zachäus, F. F. Abdi, L. M. Peter, R. van de Krol, *Chem. Sci.* **2017**, *8*, 3712–3719.

[10] X. Chang, T. Wang, P. Zhang, J. Zhang, A. Li, J. Gong, *J. Am. Chem. Soc.* **2015**, *137*, 8356–8359.

[11] a) J. A. Seabold, K. S. Choi, *J. Am. Chem. Soc.* **2012**, *134*, 2186–2192; b) K. J. McDonald, K.-S. Choi, *Energy Environ. Sci.* **2012**, *5*, 8553–8557; c) T. W. Kim, K.-S. Choi, *Science* **2014**, *343*, 990–994; d) T. W. Kim, Y. Ping, G. A. Galli, K. S. Choi, *Nat. Commun.* **2015**, *6*, 8769; e) B. Zhang, L. Wang, Y. Zhang, Y. Ding, Y. Bi, *Angew. Chem. Int. Ed.* **2018**, *57*, 2248–2252; *Angew. Chem.* **2018**, *130*, 2270–2274.

[12] T. Li, T. Kasahara, J. He, K. E. Dettelbach, G. M. Sammis, C. P. Berlinguette, *Nat. Commun.* **2017**, *8*, 390.

[13] J. K. Cooper, S. Gul, F. M. Toma, L. Chen, P.-A. Glans, J. Guo, J. W. Ager, J. Yano, I. D. Sharp, *Chem. Mater.* **2014**, *26*, 5365–5373.

[14] D. Kang, T. W. Kim, S. R. Kubota, A. C. Cardiel, H. G. Cha, K. S. Choi, *Chem. Rev.* **2015**, *115*, 12839–12887.

[15] A. M. Couper, D. Pletcher, F. C. Walsh, *Chem. Rev.* **1990**, *90*, 837–865
[16] M. W. Kanan, D. G. Nocera, *Science* **2008**, *231*, 1072–1075.
[17] G. M. Carroll, D. R. Gamelin, *J. Mater. Chem. A* **2016**, *4*, 2986–2994.
[18] J. Qiu, H. Hajibabaei, M. R. Nellist, F. A. L. Laskowski, S. Z. Oener, T. W. Hamann, S. W. Boettcher, *ACS Energy Lett.* **2018**, 961–969.
[19] P. J. Cameron, L. M. Peter, S. Hore, *J. Phys. Chem. B* **2005**, *109*, 930–936.
[20] A. J. Bard, L. R. Faulkner, *Electrochemical Methods: Fundamentals and Applications*, 2nd ed., John Wiley & Sons, Inc., **2001**.
[21] D. Eisenberg, H. S. Ahn, A. J. Bard, *J. Am. Chem. Soc.* **2014**, *136*, 14011–14014.
[22] L. M. Peter, K. G. U. Wijayantha, A. A. Tahir, *Faraday Discuss.* **2012**, *155*, 309–322.
[23] Y. Ma, S. R. Pendlebury, A. Reynal, F. Le Formal, J. R. Durrant, *Chem. Sci.* **2014**, *5*, 2964–2973.
[24] a) B. Klahr, S. Gimenez, F. Fabregat-Santiago, J. Bisquert, T. W. Hamann, *J. Am. Chem. Soc.* **2012**, *134*, 16693–16700; b) Y. Ma, A. Kafizas, S. R. Pendlebury, F. Le Formal, J. R. Durrant, *Adv. Funct. Mater.* **2016**, *26*, 4951–4960.
[25] a) M. Rafiee, B. Karimi, S. Alizadeh, *ChemElectroChem* **2014**, *1*, 455–462; b) B. Karimi, M. Ghahremani, R. Ciriminna, M. Pagliaro, *Org. Process Res. Dev.* **2018**, *22*, 1298–1305.

Manuscript received: March 20, 2019
Accepted manuscript online: May 31, 2019